ACS APPLIED MATERIALS & INTERFACES

Research Article

www.acsami.org

Increasing Crystallinity for Improved Electrical Conductivity of TiO_2 Blocking Layers

Angela S. Wochnik, Matthias Handloser, Dajana Durach, Achim Hartschuh, and Christina Scheu*

Department Chemistry, Ludwig-Maximilians-University Munich, Butenandtstrasse 5-13, 81377 Munich, Germany

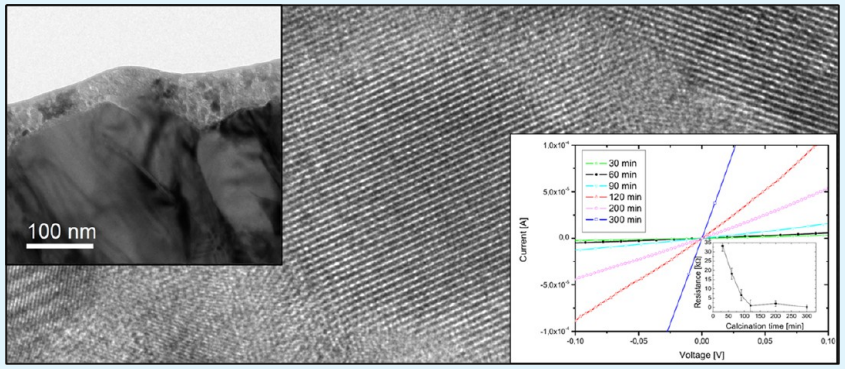

ABSTRACT: In this Research Article, we present our results on the optimization of the TiO_2 blocking layer to improve the efficiency of organic and hybrid solar cells and make them more competitive with standard silicon devices. The major aim of the present work is to increase the electrical conductivity within the TiO_2 blocking layer to guarantee for efficient charge carrier transport and separation. This is realized by optimizing the calcination processes toward an increase in particle/domain size to increase the unpercolated pathways for charge carriers and to get deeper insight into the morphology of the sol–gel produced films.

KEYWORDS: *TiO_2 blocking layer, solar cells, conductivity, morphology, sol–gel, thin films*

INTRODUCTION

In recent years titanium dioxide thin films have attracted more and more research interest because of their chemical, electrical and optical properties allowing various applications in different fields, such as microelectric devices and solar cells.[1] Especially in solar cells, such as dye sensitized or extremely thin absorber solar cells, TiO_2 thin films are applied as blocking layers to prevent short circuiting.[2−4] Numerous studies have shown that the use of a blocking layer has a positive effect on the solar cell performance.[5,6] Various techniques can be used to grow TiO_2 blocking layers such as electrodeposition,[3] magnetron-sputtering,[7] chemical vapor deposition, atomic layer deposition,[8] chemical spray pyrolysis[9,10] and the sol–gel method.[1,11] Many investigations were done on differently prepared films regarding their structure, optical and electrical properties and the influence on solar cell efficiency.[10,12,13] Also, experiments were conducted concerning the effect of layer thickness and calcination temperatures on the blocking layer performance.[1,14] The sol–gel method has some benefits compared to other techniques like controllability and reproducibility and is convenient for the preparation of nanostructured thin films because of nanometer-sized sol-particles.[15,16] This method is cheap, easy to apply and can be processed at low temperatures, which is important for manufacturing multilayered organic solar cells.[17] Different deposition methods on substrates e.g. dip and spin coating can be used.[11,18] The synthesis of TiO_2 blocking layers prepared via a sol–gel method is reported in literature with different precursors, solvents, or catalysts.[19,20] The effect of different parameters like the pH value of the sol–gel system, catalyst concentration and calcination temperature on the particle size, crystal phase or structure was investigated.[1,19,21−23] In this work, we synthesized TiO_2 blocking layers in Anatase modification via a sol–gel method, using a calcination temperature of 450 °C. The deposition on fluorine-doped tin oxide (FTO) coated glass was done by spin-coating. We show the strong influence of the dwell time during calcination on the particle size and electric conductivity of the films. The particle size within the obtained Anatase layers was characterized with high resolution transmission electron microscopy (HRTEM). In addition, the film thicknesses after spin-coating with two different speeds were investigated by transmission electron microscopy (TEM). The electrical conductivity of the blocking layers was studied via *I*–*V* measurements. The resulting enhancement of light conversion efficiency in different types of solar cells utilizing TiO_2 blocking layers can be found elsewhere.[2,6]

Received: March 27, 2013
Accepted: May 28, 2013
Published: May 28, 2013

EXPERIMENTAL METHODS

All used chemicals were of analytical grade and used without further purification. Fluorine-doped tin oxide conductive glass (Pilkington) with a dimension of 20 × 15 × 2 mm^3 was taken as substrate for the deposition of the TiO_2 films. The FTO was ultrasonicated in a solution of one part extrane and five parts double-distilled water for 15 min. A second ultrasonication was done with ethanol for another 15 min. Afterward, the substrates were dried with compressed air and treated in an O_2-plasma cleaner for 10 min. For the synthesis of the TiO_2 layers a modified version of the synthesis route of Mandlmeier et al.[20] was used. A highly diluted tetrahydrofuran sol−gel solution was prepared by adding 0.186 mL of concentrated hydrochloric acid to 0.275 mL of tetraorthoethyltitanate, while stirring and diluting the incurred sol−gel solution with 3.5 mL of tetrahydrofuran. For the deposition of the TiO_2 layers on the cleaned FTO substrates, a spin coater was used. The prepared sol−gel solution (0.130 mL) was added on the FTO substrates. The spin coating parameters were 3000 rpm for 1.5 min leading to thinner films or 1500 rpm for 1.5 min leading to thicker films. After spin coating, the layers were heated up to a temperature of 450° at a heating rate of 0.65 deg/min, kept at this temperature for 30 (film 1), 60 (film 2), 90 (film 3), 120 (film 4), 200 (film 5), and 300 (film 6) min and then cooled slowly down to room temperature within 11.0 h. The obtained TiO_2 films showed a homogeneous, transparent surface. All films synthesized with different dwell times were prepared with spin coating speeds of either 3000 or 1500 rpm. To characterize the films, different analytical techniques were applied. To get insight into morphology of the TiO_2 according film thicknesses and crystal grain sizes, a FEI Titan 80−300 (S)TEM, equipped with a Gatan Tridiem image filter and an EDAX energy dispersive X-ray (EDX) detector for analytical measurements, was used. Cross-sectional TEM specimens were prepared as described by Strecker et al.[24] Electron diffraction experiments were performed to determine the crystal phase of the film. The data were evaluated using a calibrated camera constant obtained using a Si standard leading to high accuracy (error of less than 2%). To investigate the conductivity of the films, *I*−*V* curves were measured with a Keithley source-meter 2636a.

RESULTS AND DISCUSSION

TEM measurements were performed to investigate the influence of the different calcination times on the structure of the TiO_2 films prepared at 450 °C and to determine the thickness of the films with different spin coating parameters. Figure 1 shows exemplary TEM bright field images of two films. The bright field images in Figure 1 display film 4 (a), which was left at 450 °C for 120 min and spin coated with 3000 rpm, and film 6 (b) left at 450 °C for 300 min and spin coated with 1500 rpm. It can be seen that the films are polycrystalline.

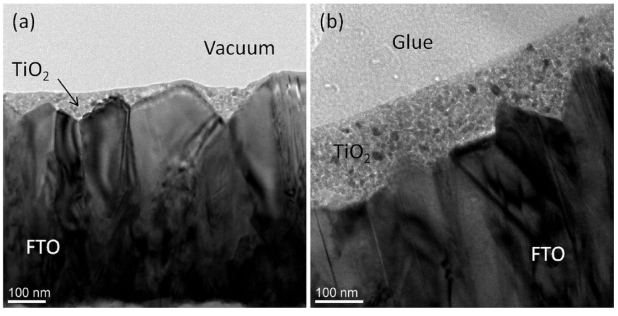

Figure 1. (a) TiO_2 film spin coated at 3000 rpm. The resulting layer thickness is between 14−20 nm in thinner regions. The film depicted in panel b was spun at 1500 rpm and increased in thickness by a factor of 4 compared to that in panel a.

In our case the local roughness of the FTO substrate was around 50−75 nm. The relativley high surface roughness of the FTO substrate is due to the fabrication process (CVD method).[25] In contrast the prepared TiO_2 film shows a flat surface. Furthermore, it can be observed that the thinner film (Figure 1a) only fills the gaps of the rough FTO surface and exhibits a minimum film thickness of about 14−20 nm and a maximum thickness of about 100 nm, while the film shown in Figure 1b, which was spin coated with 1500 rpm shows a minimum film thickness of about 70−75 nm and a maximum film thickness of about 180 nm. This can be attributed to higher spin coating speeds resulting in higher centripetal forces, removing excess material. To investigate the influence of the different calcination times on the grain size in the films HRTEM images were realized. Examples are shown in figure 2. In figure 2 (a) film 1, (b) film 2, (c) film 3, (d) film 4, (e) film 5, and (f) film 6 is depicted. All films are polycrystalline, with the crystal grains embedded in an amorphous matrix.

An orientation relationship with the FTO substrate could not be found. The analysis of the average grain size of the different films was obtained from cross sectional HRTEM images depicted in figure 2. They increase from 8.9 ± 0.5 nm to 13.1 ± 0.5 nm for film 1 to film 6. The values for the diameter correspond to the maximum length of the particles. The obtained measurement error represents the standard deviation obtained by analyzing several HRTEM images. These results indicate that longer calcination times lead to increased grain sizes within the films. In Figure 3, the grain sizes are plotted against the calcination times. It can be seen that the grain size in the first four films follows an almost linear behavior, indicating continuous growth. Further investigations of the HRTEM images reveals that the film 1−4 show amorphous areas between the grains which are no longer observed in film 5 (calcination time 200 min). This indicates that the crystal grains grow into the amorphous areas explaining the decrease in growth speed at a certain point.

The diffraction pattern next to Figure 2c was taken at film 3 and film 6 (next to Figure 2f) from an aperture of about 150 nm diameter. The pattern proves that the film is polycrystalline, without a preferred orientation and shows the (101), (112), (200), (211), and (204) reflections of TiO_2 in the Anatase modification. Beside reflections of the FTO substrate no additional reflections related to impurities or other TiO_2 modifications were found. The analysis of the diffraction pattern taken from the films 1−6 showed the same results. However, a diffuse scattering in the diffraction patterns of films 1−4 is observed which is due to the amorphous matrix.

To correlate electrical resistance and grain size within the TiO_2 film, *I*−*V* curves of films prepared with a spin coating speed of 1500 rpm were acquired. Several films from each calcination times were measured. Example *I*−*V* curves for different calcination times are displayed in Figure 4. For the *I*−*V* measurements, the TiO_2 film thickness was kept constant at 180 nm (max. thickness) to reduce the risk of creating short circuits by contacting the sample, which were observed regularly in the thin films. The inset in Figure 4 shows the resulting resistance for each calcination time. The extracted resistances correspond with the measured grain size within the film (see Figure 3). With linear increasing grain size the resistance drops also linearly. After a calcination time of approximately 120−200 min the minimum value for the resistance is reached. This is exactly where the biggest grain sizes have been recorded (see Figure 3).

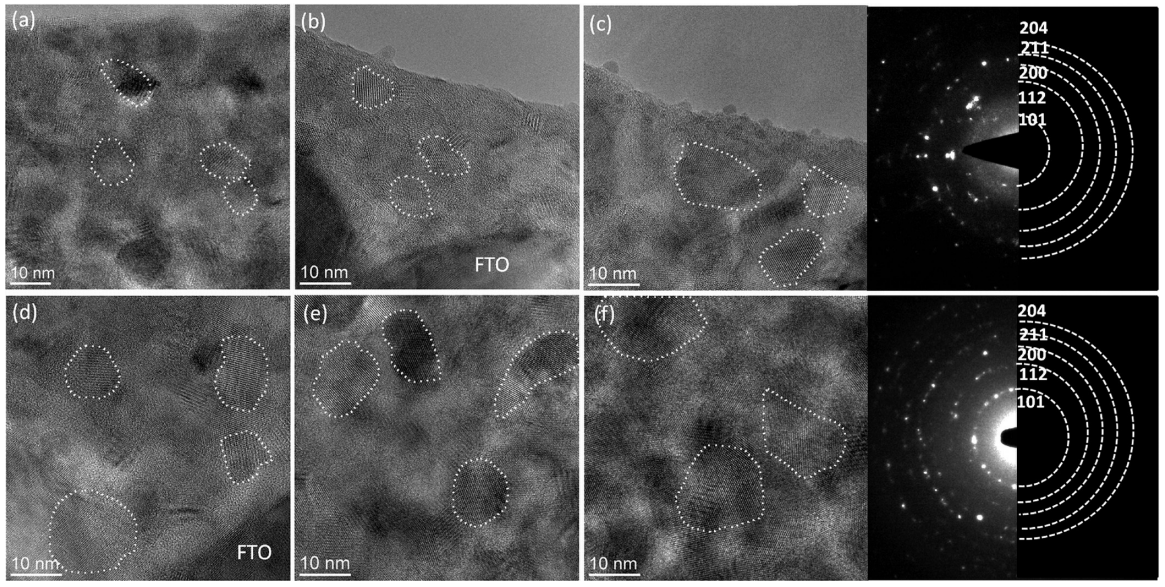

Figure 2. From panels a–f, the calcination time is increased from 30 to 300 min. In every HRTEM image some respective particles are labeled by a white ring as a guide to the eye. With increasing calcination time the particle size increases from 8.9 to 13.1 nm in average. The diffraction pattern next to panels c and f show reflections of TiO_2 in Anatase modification belonging to (101), (112), (200), (211), and (204) lattice planes of film 3 (next to panel c) and film 6 (next to panel f). The patterns were taken with an aperture with an diameter of 150 nm. Each film has the same maximum film thickness of ∼100 nm.

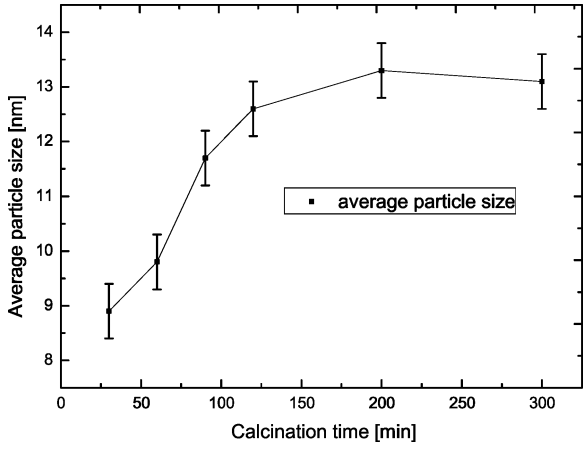

Figure 3. Grain size (14–20 nm) within the thin TiO_2 film increases with calcination time. From 30 to 120 min, an almost linear increase in size with time is visible. The deviation from the linear increase in particle size toward saturation is because of the reduced amount of amorphous areas between the crystal grains (see text).

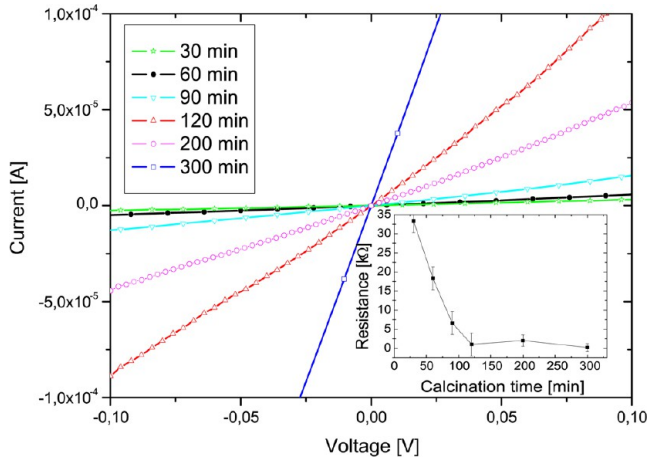

Figure 4. *I*–*V* characteristics of different TiO_2 films. Every film consists of the same thickness. The calcination time is increased from 30 to 300 min. The inset shows the calculated resistance of each film. Here the resistance drops linearly for calcination times of 30–120 min.

The results show that a longer dwell time at 450 °C during the calcination of the TiO_2 films leads to an increase of the grain size and consequently to an increase of the conductivity. Also the decrease of the amorphous areas in the films can have an influence on the improved conductivity. Our results are in good accordance with quantum mechanical calculations of polycrystalline metallic materials by Reiss et al.[26] They showed an exponential decrease of the calculated conductivity with respect to the number of grain boundaries per mean free path. Their calculations are in good agreement with an empirical model proposed by Vancea et al.[27,28] which is based on experimental investigations of Cu, Al, Ag, Au, Ni, and Pt films. Sun et al.[14] investigated the effect of the film thickness on the power conversion efficiency of TiO_2 blocking layers of organic solar cells. The TiO_2 layers were synthesized by spray pyrolysis at a temperature of 450 °C. Resistance analysis of their films revealed that charge transport is not limited even for 500 nm thick films but that the light intensity limits the device's performance. They found an optimal thickness of 100 nm for their investigated solar cells. In our work, this thickness could be reached with a spin coating speed of 1500 rpm. The conductivity seems not to be influenced by the film thickness but we found that it can be increased by the calcination time. We propose that a higher conductivity of the TiO_2 blocking layers should have a positive influence on the solar cell performance. This should be further investigated in different types of solar cells for example extremly thin absorber, thin film, or organic solar cells.

CONCLUSION

In conclusion, six different TiO_2 films were prepared with a sol−gel synthesis and deposited on FTO substrates by spin coating and calcinating with varying dwell times (30, 60, 90, 120, 200, and 300 min) at 450 °C. TEM investigations were realized focusing on the grain size and the crystal phase of the FTO. Additionally, investigations on the influence of the spin coating speed on the film thickness were done. Bright field images reveal a thickness of 14−20 nm in the thinnest region for films prepared with a faster spin coating speed (3000 rpm) and 70−75 nm for films prepared with a slower spin coating speed (1500 rpm). Furthermore these bright field TEM images show a good adaption of the TiO_2 films to the rough surface of the FTO substrate and that they have a flat surface. Electron diffraction experiments reveal TiO_2 in Anatase modification for all films. No reflections which indicate impurities were found. Additionally the electron diffraction pattern indicates polycrystallinity and the presence of an amorphous phase for dwell times ≤120 min. The investigations of the HRTEM images show a random orientation without preference of the grains. The analysis of the HRTEM images regarding the grain size in the films with different dwell times yielded in an increase from 8.9 ± 0.5 nm for film 1 (30 min) to 13.1 ± 0.5 nm for film 6 (300 min). Also a decrease of amorphous areas between the grains with longer dwell times can be observed. Following these findings *I*−*V* curves were measured to investigate the influence of the grain size on the conductivity of the films. Our results show an increase of the particle size with longer dwell time at 450 °C during the calcination and a simultaneous decrease of amorphous areas between the particles up to calcination times of 120−200 min. Consequently an increase of the conductivity with an increase of particle size of the layers was observed. After 120 min, no significant increase of grain size is detected (Figure 3). An optimum balance between resistance and grain size is reached after 120−200 min, which leads to an increase in electrical conductivity by a factor of ∼150 compared to the shortest dwell time. We propose that a calcination time of more than 120 min increases the efficiency of organic and hybrid organic solar cells utilizing TiO_2 blocking layer.

AUTHOR INFORMATION

Corresponding Author

*E-mail: Christina.Scheu@cup.uni-muenchen.de.

Notes

The authors declare no competing financial interest.

ACKNOWLEDGMENTS

Financial support from the Deutsche Forschungsgemeinschaft (DFG) through the cluster of excellence Nanosystems Initiative Munich (NIM) as well as the "Identification and overcoming of loss mechanisms in nanostructured hybrid solar cells - pathways towards more efficient devices" project. Technical support from Steffen Schmidt, Florian Auras and Alexander Müller is gratefully acknowledged.

REFERENCES

(1) Ahn, Y. U.; Kim, E. J.; Kim, H. T.; Hahn, S. H. *Mater. Lett.* **2003**, *57*, 4660−4666.
(2) Yu, H.; Zhang, S.; Zhao, H.; Will, G.; Liu, P. *Electrochim. Acta* **2009**, *54*, 1319−1324.
(3) Jang, K.-I.; Hong, E.; Kim, J. H. *Korean J. Chem. Eng* **2012**, *29*, 356−361.
(4) Lenzmann, F.; Nau, M.; Kijatkina, O.; Belaidi, A. *Thin Solid Films* **2004**, *451*−*452*, 639−643.
(5) Burke, A.; Ito, S.; Snaith, H.; Bach, U.; Kwiatkowski, J.; Grätzel, M. *Nano Lett.* **2008**, *8*, 977−981.
(6) Cho, T.-Y.; Yoon, S.-G.; Sekhon, S.-S.; Kang, M. G.; Han, C.-H. *Bull. Korean Chem. Soc.* **2011**, *32*, 3629−3633.
(7) Yildiz, A.; Lisesivdin, S. B.; Kasap, M.; Mardare, D. *J. Non-Cryst. Solids* **2008**, *354*, 4944−4947.
(8) Aarik, J.; Aidla, A.; Kiisler, A.-A.; Uustare, T.; Sammelselg, V. *Thin Solid Films* **1997**, *305*, 270−273.
(9) Cameron, P.; Peter, L. *J. Phys. Chem. B* **2003**, *107*, 14394−14400.
(10) Peng, B.; Jungmann, G.; Jäger, C.; Haarer, D.; Schmidt, H.-W.; Thelakkat, M. *Coord. Chem. Rev.* **2004**, *248*, 1479−1489.
(11) Mechiakh, R.; Ben Sedrine, N.; Chtourou, R.; Bensaha, R. *Appl. Surf. Sci.* **2010**, *257*, 670−676.
(12) Handloser, M.; Dunbar, R.; Altpeter, P.; Scheu, C.; Schmidt-Mende, L.; Hartschuh, A. *Nanotechnology* **2012**, *23*, 305402−305408.
(13) Jiang, C.; Leung, M.; Koh, W. L.; Li, Y. *Thin Solid Films* **2011**, *519*, 7850−7854.
(14) Sun, H.; Weickert, J.; Hesse, H.; Schmidt-Mende, L. *Sol. Energy Mater. Sol. Cells* **2011**, *95*, 3450−3454.
(15) Hu, L.; Yoko, T.; Kozuka, H.; Sakka, S. *Thin Solid Films* **1992**, *219*, 18−23.
(16) Chrysicopoulou, P.; Davazoglou, D.; Trapalis, C.; Kordas, G. *Thin Solid Films* **1998**, *323*, 188−193.
(17) Hench, L. L.; West, J. K. *Chem. Rev.* **1990**, *90*, 33−72.
(18) Chang, C.; Cheng, L.; Lin, C.; Yu, Y. *J. Sol-Gel Sci. Technol.* **2012**, *63*, 30−35.
(19) Hu, Y.; Tsai, H.; C.L., H. *Mater. Sci. Eng.* **2003**, *A344*, 209−214.
(20) Mandlmeier, B.; Szeifert, J.; Fattakhova-Rohlfing, D.; Amenitsch, H.; Bein, T. *J. Am. Chem. Soc.* **2011**, *133*, 17274−17282.
(21) Rawolle, M.; Niedermeier, M. A.; Kaune, G.; Perlich, J.; Lellig, P.; Memesa, M.; Cheng, Y.-J.; Gutmann, J. S.; Müller-Buschbaum, P. *Chem. Soc. Rev.* **2012**, *41*, 5131−5142.
(22) Orilall, M. C.; Wiesner, U. *Chem. Soc. Rev.* **2011**, *40*, 520−535.
(23) Rawolle, M.; Braden, E. V.; Niedermeier, M. A.; Magerl, D.; Sarkar, K.; Fröschl, T.; Hüsing, N.; Perlich, J.; Müller-Buschbaum, P. *Chem. Phys. Chem.* **2012**, *13*, 2412−2417.
(24) Stecker, A.; Salzberger, U.; Mayer, J. *Prakt. Metallogr.* **1993**, *30*, 482−495.
(25) Yang, Y.; Wang, L.; Yan, H.; Marks, T. J.; Li, S. *Appl. Phys. Lett.* **2006**, *89*, No. 051116.
(26) Reiss, G.; Vancea, J.; Hoffmann, H. *Phys. Rev. Lett.* **1986**, *56*, 2100−2103.
(27) Vancea, J.; Hoffmann, H.; Kastner, K. *Thin Solid Films* **1984**, *121*, 201−216.
(28) Vancea, J.; Hoffmann, H. *Thin Solid Films* **1982**, *92*, 219−225.